Effect of pH in syngas conversion to C4 & C6 acids in mixed-culture trickle bed reactors

Biomass and Bioenergy 187 (2024) 107292

Contents lists available at ScienceDirect

Biomass and Bioenergy

journal homepage: www.elsevier.com/locate/biombioe

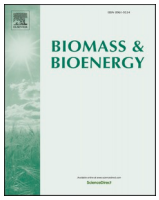

Effect of pH in syngas conversion to C4 & C6 acids in mixed-culture trickle bed reactors

Cesar Quintela [a], Antonio Grimalt-Alemany [a], Oskar Modin [b], Yvonne Nygård [c], Lisbeth Olsson [c], Ioannis V. Skiadas [a], Hariklia N. Gavala [a,*]

[a] Department of Chemical and Biochemical Engineering, Technical University of Denmark, 2800, Kgs. Lyngby, Denmark
[b] Division of Water Environment Technology, Department of Architecture and Civil Engineering, Chalmers University of Technology, Gothenburg, Sweden
[c] Division of Industrial Biotechnology, Department of Life Sciences, Chalmers University of Technology, Gothenburg, Sweden

ARTICLE INFO

Keywords:
Syngas fermentation
Butyric acid
Caproic acid
Chain elongation
Reverse beta oxidation
Trickle bed reactor

ABSTRACT

Syngas fermentation allows for the conversion of wastes into useful commodity chemicals. To target higher value products, the conditions can be tuned to be favourable for both acetogenic and reverse beta-oxidation pathways and produce, in one stage, butyric and caproic acid. Studies in CSTR have shown the crucial role of pH, which must be low enough to allow for ethanol generation in the acetogenic step while avoiding the inhibition of reverse β-oxidation in acidic conditions. However, no studies have investigated the effect of pH in reactor configurations suitable for syngas fermentation (i.e., allowing for cell retention and exhibiting high mass transfer rates at low operating costs), such as Trickle Bed Reactors, TBR. In this study, two TBR were used to study the pH effect on the fermentation of syngas to produce C4 and C6 acids, using undefined mixed cultures. Five pH values were tested in the range 4.5–7.5, and pH 6 was found to be the most favourable for simultaneous production of C4 & C6 acids from syngas, which agrees with what was found in suspended growth systems. In addition, the highest titers in literature so far were achieved in the TRB. 16S rRNA analysis was performed showing *Clostridium* and *Rummenliibacillus* to be the key genus for the efficient process at pH 6. Finally, the experimental methodology followed, and data collected proved the robustness of mixed culture biofilm reactors in respect to pH changes, as the same reactor performance and bacterial community were achieved regardless of the operation history.

1. Introduction

The sixth Intergovernmental Panel on Climate Change (IPCC) report, released between 2021 and 2023 [1], stressed that as the global temperature continues rising, extreme events such as floods, fires, and droughts will increase in frequency and intensity, with some impacts being already irreversible. To limit the severity of future scenarios, IPCC urged policymakers to implement massive and immediate cuts in greenhouse gases emissions. Industries must therefore shift towards circular economy models, minimizing waste generation and extractive processes. Syngas fermentation, by combining thermochemical and biological methods (gasification and fermentation), allows for (1) full conversion of waste into chemicals, in contrast to direct fermentation where a recalcitrant waste fraction is usually left unfermented; and (2) mild operating conditions and resistance to inhibitors and gas feed composition changes when compared to chemical catalysis [2]. These properties make it an attractive technology to be used in the context of the chemical industry transition. Syngas fermentation has been commercialized to produce ethanol [3], while pilot scale CO_2 and syngas biomethanation has also recently proven successful [4,5]. In recent years, the production of volatile fatty acids (VFA) with more than two (2) carbon atoms from syngas through chain elongation has gained increased attention for their use as platform or commodity chemicals [6]. However, to compete with the prices of the respective fossil-based chemicals, fermentation processes should undergo significant cost reductions. Undefined mixed-culture fermentations operate without the sterilization costs of pure and co-culture fermentations and can be run in cost-effective continuous fermentations (as opposed to batch). They have therefore been proposed to be key for next-generation biofuels and commodity (bulk) chemicals production [7–10]. Therefore, production of C4 and C6 acids from syngas via chain elongation by mixed microbial consortia is a very attractive alternative to fossil-based production processes.

The process to obtain butyric, caproic, and other even-numbered

* Corresponding author.
E-mail addresses: hnga@kt.dtu.dk, hari_gavala@yahoo.com (H.N. Gavala).

https://doi.org/10.1016/j.biombioe.2024.107292
Received 12 March 2024; Received in revised form 28 May 2024; Accepted 22 June 2024
Available online 2 July 2024

carboxylic acids from syngas, consists of two steps. First, syngas is converted by acetogenic bacteria to acetic acid and ethanol through the Wood-Ljungdahl pathway; and then ethanol is used by the chain elongating microbes to elongate acetic and the subsequent acids by two carbons via the reverse β-oxidation pathway. Although some acetogens can directly convert syngas into butyric acid, very few species have been reported so far to produce caproic acid from syngas [11], and their yields are usually low with 20–40 % of carbon in the products present in butyric and caproic acid [12,13]. Additionally, genetic engineering approaches have not been able yet to improve the performance of wild strains for this process [11,14]. On the contrary, defined co-cultures and undefined mixed cultures benefit from microbes specialized in a single step of the process and thus have achieved better yields than wild-type pure cultures. Diender et al. [15] established a synthetic co-culture in which *C. autoethanogenum* converted CO to acetic acid and ethanol, and *C. Kluyveri* elongated them to butyric and caproic acid, leading to 47 % of the carbon in the products present in the elongated acids. In another study, Wang et al. [16] inoculated with a mixed culture a hollow-fiber membrane biofilm reactor operated in batch mode and reached 75 % of the carbon present in butyric and caproic acid. Nevertheless, the optimization of mixed culture fermentations can be more challenging, as a compromise between the optimal growth conditions for the different strains involved in the conversion process must be found. Additionally, in the case of undefined mixed cultures, the conditions chosen must favour the microbes involved in the conversion as well as inhibit unwanted competing reactions [17–19].

One of the most crucial parameters influencing acetogenesis and chain elongation is the pH. In the acetogenic step, acetic acid is the initial product of the Wood-Ljungdahl pathway, while ethanol is subsequently produced from acetic acid with the cost of Fd_{red} and the reduced form of nicotinamide adenine dinucleotide, NADH [20]. Reaction 1 refers to acetic acid production from CO_2 and H_2, while reactions 2 and 3 and refer to ethanol production from acetic acid, and CO_2 and H_2, respectively. For a more complete set of reactions with acetic acid and ethanol production also from CO the reader can refer to the publication of Grimalt-Alemany et al. [21]. Acetic acid is generally a more favourable product, since it allows for more adenosine triphosphate, ATP, production per mol of gaseous substrate consumed. However, certain conditions such as low pH or high acetic acid concentrations, have been shown to trigger solventogenesis, i.e. conversion of acids to alcohols, to avoid undissociated acids to re-enter the cells and uncouple the proton motive force from ATP generation [22–24]. Regarding the chain elongation step, several studies have reported the reverse β-oxidation pathway to be promoted by neutral to high pH (6–7.5) and to usually be inhibited at pH below 5 [25,26]. This is presumably because the reverse β-oxidation reaction promotes an increase in the number of acid molecules when ethanol is the electron donor (reaction 4), and a higher ratio of undissociated acids (as longer carboxylic acids have a higher pKa), both resulting in higher concentrations of undissociated acids. Therefore, for simultaneous acetogenesis and chain elongation, a pH compromise that satisfies the ethanol production requirement (low enough pH), and the chain elongation requirements (high enough pH), must be met [25].[20,27].

$$2\,CO_2 + 4\,H_2 \rightarrow\ C_2H_4O_2 + 2\,H_2O \quad (1)$$

$$C_2H_4O_2 + 2\,H_2 \rightarrow\ C_2H_6O + H_2O \quad (2)$$

$$2\,CO_2 + 6\,H_2 \rightarrow\ C_2H_6O + 3\,H_2O \quad (3)$$

$$6\,C_2H_6O + 4\,C_2H_4O_2 \rightarrow 5\,C_4H_8O_2 + 4\,H_2O + 2\,H_2 \quad (4)$$

All studies reviewed dealing with the effect of pH in simultaneous syngas fermentation and chain elongation were performed in continuously stirred tank reactors (CSTR) [25,28] or serum bottles [29]. However, these set-ups require high operational costs at industrial scale to disperse the gas bubbles and reach satisfactory mass transfer rates of the gaseous substrates into the liquid. In addition, the low biomass yields of acetogenic cultures typically result in low biomass concentration and conversion rates, if no cell retention or recycling is applied. Trickle Bed Reactors (TBRs), on the other hand, allow the formation of biofilm, thus increasing biomass retention, and exhibit high gas-to-liquid mass transfer rate at a very low operational cost [30]. Due to the physiological heterogeneity in biofilms (which result from gas composition, nutrients, pH, and other concentration gradients) the characteristics (performance, microbial community composition, and response to operational parameters) of biofilm reactors could be significantly different, compared to those of suspended growth reactors [31–33]. Despite this, the pH effect on the performance of microbes in TBRs or other biofilm reactors has not been investigated yet.

The aim of our study was to elucidate the effect pH has on the TBR microbial communities (both in suspension and biofilm) and their performance, as well as to investigate whether this effect is independent on the operational history of the reactor under different pH values. Our underlying hypotheses were that microbial consortia and their metabolic response will change because of the operating pH, in turn influencing the conversion performance of the TBR. Additionally, it was hypothesized that microbial community changes caused by different operating pH, and thus the TBR performance changes, will be reversible within a certain pH range. Five different pH values were tested (4.5, 5.3, 6, 6.8, and 7.5) in two TBRs fed with syngas, with continuous monitoring of the gas consumption and liquid products generation. The pH range 4.5–7.5 was chosen based on literature knowledge about chain elongation (i.e., that reverse β-oxidation pathway is known to be promoted by neutral to high pH, 6–7.5, and is usually inhibited at pH below 5) with three (3) more intermediate pH values tested to obtain more detailed knowledge about the pH effect on chain elongation in TBRs. Moreover, 16S rRNA analysis was performed, for the suspended and attached communities at each steady-state pH condition.

2. Materials and methods

2.1. Growth medium

A modified basal anaerobic (BA) medium was fed into the reactor, to supply the culture with the necessary nutrients for microbial growth. As described by Grimalt-Alemany [34], the following stock solutions were prepared: 1) macronutrients (NH_4Cl, 100 g L^{-1}; NaCl, g L^{-1}; $MgCl_2{\cdot}6H_2O$, 10 g L^{-1}; $CaCl_2{\cdot}2H_2O$, 5 g L^{-1}), 2) dipotassium hydrogen phosphate solution ($K_2HPO_4{\cdot}3H_2O$, 200 g L^{-1}), 3) sodium sulfate solution (Na_2SO_4, 100 g L^{-1}), 4) sodium sulfide solution (Na_2S, 24.975 g L^{-1}), 5) vitamin solution (biotin, 10 mg L^{-1}; folic acid, 10 mg L^{-1}; pyridoxine HCl, 50 mg L^{-1}; riboflavin HCl, 25 mg L^{-1}; thiamine HCl, 25 mg L^{-1}; cyanocobalamin, 0.5 mg L^{-1}; nicotinic acid, 25 mg L^{-1}; *p*-aminobenzoic acid, 25 mg L^{-1}; lipoic acid, 25 mg L^{-1}; d-pantothenic acid hemicalcium salt, 25 mg L^{-1}), and 6) modified ATCC 1754 trace metal (micronutrients) solution (nitrilotriacetic acid, 2000 mg L^{-1}; $MnSO_4{\cdot}H_2O$, 1119 mg L^{-1}; $Fe(SO_4)_2(NH_4)_2{\cdot}6H_2O$, 800 mg L^{-1}; $CoCl_2{\cdot}6H_2O$, 200 mg L^{-1}; $ZnSO_4{\cdot}7H_20$, 200 mg L^{-1}; $CuCl_2{\cdot}2H_2O$, 20 mg L^{-1}; $NiCl_2{\cdot}6H_20$, 20 mg L^{-1}; $Na_2MoO_4{\cdot}2H_2O$, 20 mg L^{-1}; $Na_2SeO_3{\cdot}5H_2O$, 27 mg L^{-1}; $Na_2WO_4{\cdot}2H_2O$, 25 mg L^{-1}; H_3BO_3, 10 mg L^{-1}; $AlCl_3$, 10 mg L^{-1}). To prepare the modified BA medium, these stock solutions were added to deionized water in the following amounts: macronutrients, 20 ml L^{-1}; dipotassium hydrogen phosphate solution, 5 ml L^{-1}; sodium sulfate solution, 10 ml L^{-1}; sodium sulfide solution, 0.2 ml L^{-1}; vitamin solution, 10 ml L^{-1}; and trace metal solution, 10 ml L^{-1}. Yeast extract was also supplemented to the media to a final concentration of 0.5 g L^{-1}. There was only one difference from Ref. [34]: the Na_2S stock solution usage was reduced four times, to achieve a final concentration of 1 ml L^{-1} in the media. This was done to avoid precipitation and darkening of the media and the reactor, which would hinder monitoring of the biofilm formation and OD measurements. All chemicals were purchased from Sigma Aldrich (Germany). Inorganic

compounds were of ACS grade, vitamins had a purity higher than 98 % and yeast extract was of microbiological grade.

2.2. Reactor configuration

Two TBRs were conceptualized and custom-built for this study, according to the process flow sheet shown in Fig. 1, and based on the reactors designed by Asimakopoulos [35], with a few modifications. The gas flow into the airtight TBR columns was controlled by mass flow controllers (Bronkhorst, Netherlands). The empty bed volume (EBV) of the TBR columns was 300 ml. The TBR columns (Figs. 1 and 3) were filled with polypropylene/polyethylene packing material (BioFLO 9—Smoky Mountain Biomedia, USA) and the liquid working volume of the TBR system (column and reservoir) was 400 ml (corresponding mainly to the volume of the liquid reservoir as the liquid retained on the surface of the packing material in the column was minimal). Liquid was continuously recirculated from the reservoir to the top of the column with a peristaltic pump (Watson Marlow, UK). Liquid media was continuously added to the system by a pump connected to a timer, set to three feeding pulses per day, and the effluent exited the system through a liquid level placed at the reservoir., The remaining gas after flowing through the column was entering the headspace of the reservoir (also anaerobically sealed), after which it exited the system through the liquid level, pumped out by the gas pressure inside the reactor. The gas was then flowing through a gas sampling port and a gas trap before being vented out inside a fume hood. Gas traps, consisting of an empty sealed flask between the outlet port and the effluent bottle, were added to the systems to prevent air from going inside the reactors at points where the gas consumption increases. A pH control system was added, consisting of a pH electrode (Mettler Toledo, Switzerland), a pH transmitter (Knick, Germany), and two pumps connected with an acid (0.5 M HCl) and a base (5 M KOH) solution, which were pumped into the reservoir. Instead of using a gas flowmeter at the reactor's gas exit, the gas flow out was calculated from the N_2 percentage in the outlet gas, which proved to be more accurate (Supplementary Material, S1.1.).

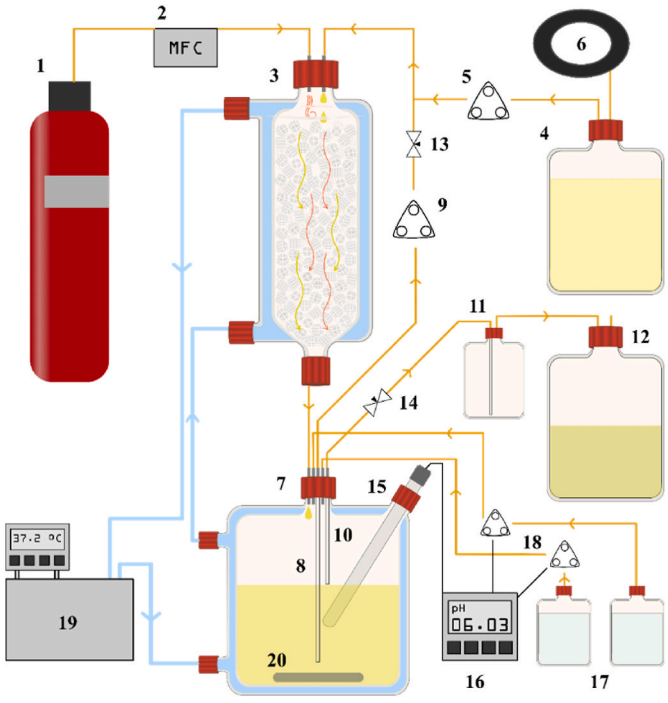

Fig. 1. Flow sheet of the TBRs set-up designed, built, and operated in this study. The main parts of the configuration are numbered in the figure, and are (1) syngas mix cylinder, (2) mass flow controller, (3) TBR, (4) liquid media, (5) liquid inflow peristaltic pump, (6) N_2 gas bag, (7) reservoir, (8) liquid tube for the recirculation (9) liquid recirculation peristaltic pump, (10) level/liquid and gas outlet tube, (11) gas trap, (12) liquid and gas effluent bottle, (13) liquid sampling port, (14) gas sampling port, (15) pH electrode, (16) pH controller, (17) acid and base solutions, (18) peristaltic pumps for acid and base solutions, (19) water bath and water jacket recirculation, and (20) stirring magnet.

2.3. Start-up and operation of the trickle bed reactors

Once mounted, two reactors (TBR1 and TBR2) were first flushed with N_2, to ensure anaerobic conditions, and then with the syngas mix used throughout the whole experiment (45 % H_2, 25 % CO_2, 20 % CO, 10 % N_2). The reactors were then filled using effluent from a syngas fermenting and chain elongating 4-L active volume CSTR fed with 25 ml min^{-1} syngas and operated at pH 6, 37 °C, and 3 days hydraulic retention time (HRT). This CSTR was originally inoculated with anaerobic sludge from the Lyngby-Taarbæk wastewater treatment plant (Denmark), which was heat pre-treated to remove methanogenic archaea, by subjecting the sludge to 95 °C for 15 min, while flushing with N_2.

For the TBRs, a start-up phase was conducted to ensure the growth of all the necessary microbial communities and to reach a steady reactor performance, which lasted for 39 days. The TBRs were started in batch operation in respect to the liquid phase, at a pH of 6, a temperature of 37 °C, a syngas flow of 1.5 ml min^{-1}, corresponding to 200 min empty bed residence time (EBRT, calculated as the TBR column EBV divided by the flowrate), and a liquid recirculation rate of 81 L $L_{EBV}^{-1}day^{-1}$. During this period, continuous operation in respect to the liquid phase was introduced with the HRT being gradually reduced to 3 days, while the syngas flow was increased to 7.5 ml min^{-1} (corresponding to 40 min EBRT, or to 33 ml min^{-1} L_{EBV}^{-1}) and the recirculation rate was increased to 2133 L L_{EBV}^{-1} day^{-1}, respectively.

The TBRs were operated at five different pH values (4.5, 5.3, 6, 6.8, and 7.5) during this study. After the start-up phase, the reactors were run at each one of the different pH set-points until the gas consumption and product profile reached a steady state, and then the pH set-point was changed to the next one. To assess the degree of variation between the reactors, TBR1 and TBR2 were operated as duplicates during the start-up phase and the first pH condition, pH 6, until they both reached a steady state. Then TBR1 was tested at pH 5.3 and 4.5 and TBR2 was tested at pH 6.8 and 7.5. At the end of the experiment, both reactors were operated again at pH 6 to ensure the results obtained at each pH were independent of the conditions tested in each reactor. The pressure of the syngas supplied and the pressure inside the reactors was set to ambient, i.e. at an absolute value of 1 atm.

2.4. Analytical techniques

Gas outflow composition was determined in a gas chromatograph (8610C, SRI Instruments, Germany) equipped with a thermal conductivity detector and two packed columns (6′ × 1/8″ Molsieve 13 × column and 6′ × 1/8″ silica gel column) connected in series through a rotating valve. The columns were kept at 65 °C for 3 min, followed by a 10 °C min^{-1} ramp till 95 °C, and a 24 °C min^{-1} ramp reaching 140 °C 50 μl gas samples were collected and injected with a gas-tight syringe (model 1750SL, Hamilton) [36]. Volatile fatty acids (VFA) and alcohols were determined through a High-Performance Liquid Chromatograph (Shimadzu, USA) equipped with a refractive index detector and an Aminex HPX-87H column (Bio-Rad, Denmark) maintained at 60 °C. 12 mM H_2SO_4 was used as eluent at a flow rate of 0.6 ml min^{-1}. The formula for calculating the e-mol distribution used in this study is detailed in the Supplementary Material (S1.2.).

The biomass concentration was indirectly monitored by measuring the optical density at a wavelength of 600 nm (OD600) using a spectrophotometer (DR3900, Hach Lange). The OD600 measurements were then correlated to the Volatile Suspended Solids concentration, or Cell Dry Weight (CDW) in the fermentation broth, according to standard

methods [37]. The pH of the broth was measured externally using a PHM210 pH meter (Hach, USA), recalibrating the internal pH electrode when necessary.

2.5. Microbial community analysis

For the analysis of the suspended communities, 10 ml liquid samples were collected at each steady-state; while for the biofilm analysis, plastic carriers carrying biofilm were collected from the upper half of the reactor in all but the first steady-state, and the biomass was washed out of the carrier, by shaking it vigorously into fresh liquid media. All samples were then centrifuged to remove the supernatant, and frozen at −20 °C for simultaneous processing at the end of the experiment.

The DNA was extracted using a DNeasy Blood and Tissue Kit (Qiagen, Denmark), and submitted to Macrogen Inc. (Korea) for 16S amplicon library preparation and sequencing using Illumina Miseq (300 bp paired-end sequencing). The libraries were constructed according to the 16S Metagenomic Sequencing Library Preparation Protocol (Part #15044223, Rev. B) using Herculase II Fusion DNA Polymerase Nextera XT Index Kit V2. Regions V4–V5 of 16S rRNA gene were amplified with primers 515F (5′-GTGYCAGCMGCCGCGGTAA-3′) and 926R (5′-CCGYCAATTYMTTTRAGTTT-3′) [38].

Raw reads were merged, quality-filtered, and denoised, using the DADA2 algorithm within the Qiime2 pipeline, to obtain amplicon sequence variants (ASVs) [39]. Taxonomic assignment was then performed using a classify-sklearn algorithm, together with a classifier trained on the Greengenes2 (2022.10) database. Further downstream analysis was performed using phyloseq and ggpubr packages in R. The raw sequences obtained in this study are available in the NCBI SRA database with BioProject accession number PRJNA1077219.

3. Results and discussion

3.1. TBR performance at different pH conditions

The two TBRs were run continuously, to test five different pH values from 4.5 to 7.5. Fig. 2 summarizes the analysed liquid effluent composition (A, B) and the gas effluent composition (C, D) profiles throughout the experiment. During the whole study, the main products were ethanol (below pH 6), acetate, butyrate, and caproate, accounting together for more than 95 % of the total e-mol in all the measured products.

The e-mol distribution in the products and the mmol day^{-1} consumption of the gaseous substrates during steady-state operation of the reactors were summarized into Fig. 3A and B, respectively. A pH of 6 appeared to be the most efficient for syngas fermentation to butyric and caproic acid. At this pH, the target products (butyric and caproic acid) accounted for 60–61 % of the total electrons in the products (Fig. 3A), and the consumption of H_2 and CO, 121.9 and 60.1 mmol day^{-1}, respectively, were also the highest measured in this study (Fig. 3B). In contrast, at pH 6.8 and pH 5.3, the chain elongation yield in the target products dropped sharply, to 31 % and 7 % e-mol, respectively, and continued decreasing at pH 4.5 and pH 7.5. These results illustrate the great impact of pH in simultaneous syngas fermentation and chain elongation processes.

The product distribution seen across the pH range applied (Fig. 3A) illustrates that for efficient production of butyric and caproic acid from syngas, a pH compromise must be found between low pH conditions, which favours ethanol production, and high pH conditions, which favours chain elongation. In this study, the most favourable pH value among the 5 values tested was found to be pH 6. Accordingly, operation at lower pH values showed very little chain elongation activity, and accumulation of unconverted ethanol; while the steady-states at higher pH conditions also showed a reduction in chain elongated products, in this case likely due to the lack of ethanol production in the acetogenic

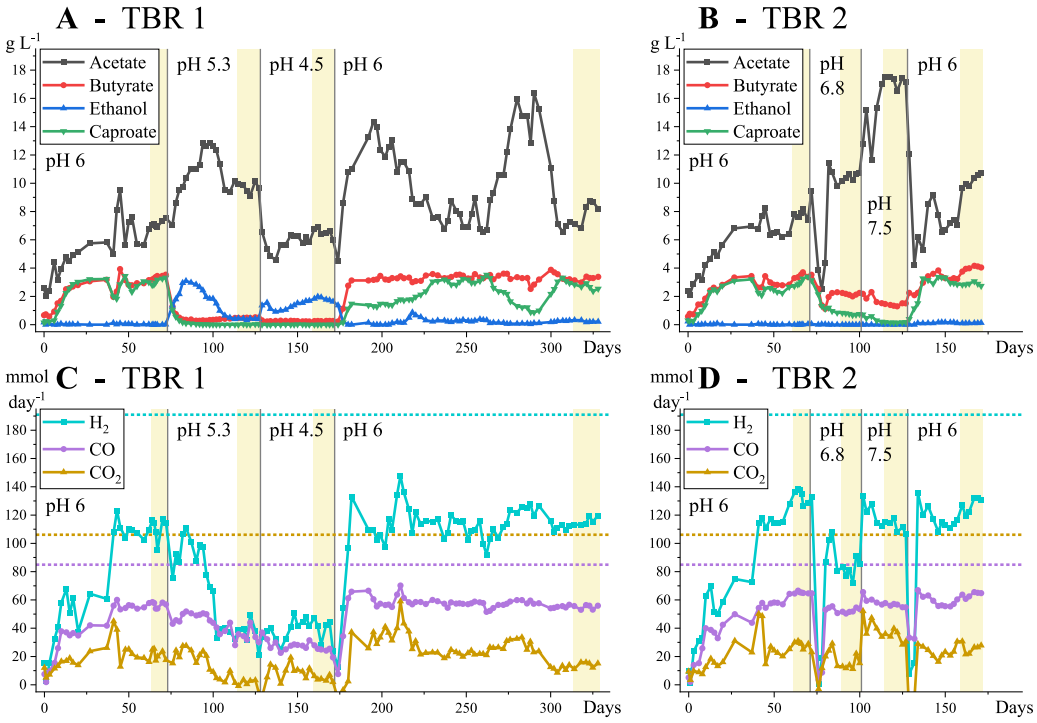

Fig. 2. Concentration in g L^{-1} of the main extracellular compounds (A and B) and overall consumption in mmol day^{-1} of the provided gaseous substrates (C and D) in TBR 1 (A and C) and TBR2 (B and D). The different pH set are indicated in the graph, and the timeframe considered for the steady-state calculations is highlighted in yellow. The inflow rates of gaseous substrates are indicated by the color-coded dotted lines in the gas consumption plots. To derive volumetric consumption rates of gas substrates and productivities of liquid products, the 0.3 L_{EBV} and 3 days HRT must be used, respectively. (For interpretation of the references to color in this figure legend, the reader is referred to the Web version of this article.)

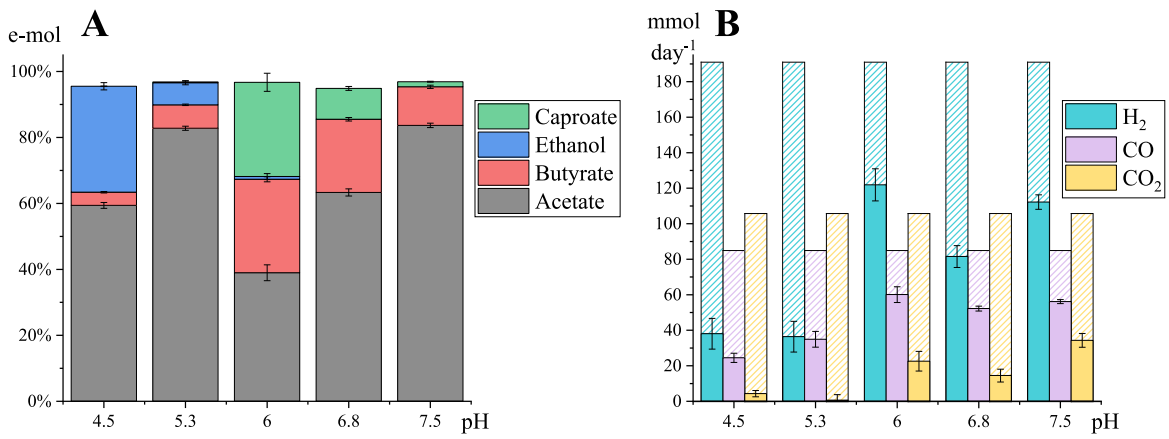

Fig. 3. Averaged e-mol distribution in the extracellular products (A) and consumption of the gaseous substrates in mmol day^{-1} (B) for each of the pH conditions tested. In plot B, the total provided gases is given in a stripe pattern, while the consumed portion is shown in a solid pattern. The e-mol distribution at pH 6 is the average of the 4 steady states reached (TBR1 and TBR2 at the beginning of the experiment and TBR1 and TBR2 at the end of the experiment), while at other pH values the average of the steady state values for each TBR is calculated. To derive volumetric gas consumption rates, the 0.3 L_{EBV} must be used.

step (Fig. 3A). Similar pH conditions have been reported in the literature for simultaneous syngas to C4 & C6 acids conversion: pH 5.5–6.5 for a *C. authoethanogenum* and *C. kluyveri* co-culture [29], and pH 5.7–6.4 for a *C. ljungdahlii* and *C. kluyveri* co-culture [28]. On the other hand, Ganigué et al. [25] reported that for simultaneous syngas fermentation and chain elongation using an undefined mixed culture, without pH control, the chain elongation activity was only inhibited when the pH of the fermentation dropped below 4.5–5. However, lower concentration of C4 & C6 acids were obtained in the study of Ganigué et al. (maximum of 0.8 g L^{-1} caproic acid) compared to the present and the two literature studies cited above, and this probably allowed the pH to drop to a lower value before the undissociated acid fraction reached an inhibitory value. Presence of chain elongation activity at lower pH conditions, as showed in the study of Ganigué et al. [25], could be beneficial to boost ethanol production even more and potentially increase C4 & C6 acid yields and productivities; however, this would entail keeping C4 & C6 acid titers low with in-line extraction tools to avoid inhibition.

Some of the transient states seen in the production profile of TBR1 (Fig. 2A), can also help in understanding the dynamics between the simultaneous processes of acetogenic and reverse β-oxidation. Particularly, around day 75 of TBR1 operation, a sharp increase of ethanol production happened together with the reduction of chain elongated products (and the increase in acetic acid production), when the pH was changed from 6 to 5.3. Ethanol productivity reached a maximum of 1.03 g L^{-1} day^{-1} with an ethanol concentration of 3.1 g L^{-1}, and then decreased progressively until a constant productivity was achieved around 0.13 g L^{-1} day^{-1} at an ethanol concentration of 0.4 g L^{-1}. Based on the stoichiometry of the chain elongation reaction, and assuming similar stoichiometries for acetic and butyric acid elongation [40], the ethanol produced by the acetogenic culture and simultaneously used in the reverse β-oxidation can be calculated as 1.2 mol ethanol per mol of butyric acid plus 2.4 mol ethanol per mol of caproic acid present. In the current study, the stoichiometric productivity of ethanol amounts to an average of 1.69 g L^{-1} day^{-1} (5.1 g L^{-1}) at pH 6. It could be hypothesized that, when the pH was changed from 6 to 5.3, the inhibition of chain elongation resulted in a transient accumulation of acetogenic products, since they were suddenly not consumed in the chain elongation reactions. Interestingly, the culture adapted to this situation by reducing the production of acetic acid, and especially ethanol, which was decreased more than 10 times. Similarly, in a co-culture study [15], the introduction of a chain elongating strain to an acetogenic pure culture producing mainly acetic acid, switched the acetogenic metabolism towards a more solventogenic state, and thus resulted in the ultimate production of chain elongated acids. This switch was caused by the removal of ethanol by the chain elongating strain, and it shows the potential synergistic effects of combining acetogenesis and chain elongation. Ultimately, the latter could also enhance gas consumption rates by removing the acetogenic products from the media.

The gas consumption was also affected by the pH (Fig. 3B) and was in fact highest at a pH of 6 when the acetogenic – reverse β-oxidation synergy took place in TBR1 (for gas consumption efficiencies, refer to Table S1 in Supplementary Material). Specifically, reducing the pH from 6 to 5.3 seemed to have a significantly negative impact on the gas consumption, which was decreased by 70, 42, and 97 % compared to the consumption at pH 6 for H_2, CO, and CO_2, respectively, and remained at similarly low levels when further reducing the pH to 4.5. In the TBR2, the increase in pH from 6 to 6.8 caused a milder gas consumption decrease of 33, 13, and 36 % compared to the consumption at pH 6 for H_2, CO, and CO_2, respectively. However, increasing the pH further to 7.5, caused the gas consumption to increase again to values similar to the ones obtained at pH 6 for H_2 and CO consumption, while CO_2 consumption at pH 7.5 was 51 % higher than that at pH 6. As it will be elaborated in the next section, different microbial communities were responsible for the acetogenic conversions at pH 6 and pH 7.5, and this could be responsible for the two most favourable pH conditions found regarding gas consumption.

To the best of our knowledge, this study resulted in the highest titers of butyric and caproic acid in a continuous syngas fermentation process (Table 1). The main reasons for it may be (1) a correct choice of pH,

Table 1
Titers (g L^{-1}) and productivities (mmol L^{-1} day^{-1}) of the main acid products at the different pH values. For pH six, the values are given as an average ± standard deviation of the four steady-states achieved.

pH	Acetic Acid		Butyric Acid		Caproic Acid	
	g L^{-1}	g L^{-1} day^{-1}	g L^{-1}	g L^{-1} day^{-1}	g L^{-1}	g L^{-1} day^{-1}
4.5	6.5 ± 0.3	2.18 ± 0.10	0.3 ± 0.0	0.09 ± 0.00	0.0 ± 0.0	0.00 ± 0.00
5.3	9.7 ± 0.3	3.23 ± 0.11	0.5 ± 0.0	0.16 ± 0.01	0.0 ± 0.0	0.00 ± 0.00
6	**8.3 ± 1.2**	**2.76 ± 0.38**	**3.5 ± 0.3**	**1.17 ± 0.10**	**2.9 ± 0.2**	**0.97 ± 0.05**
6.8	10.4 ± 0.2	3.48 ± 0.07	2.1 ± 0.1	0.72 ± 0.03	0.7 ± 0.0	0.25 ± 0.02
7.5	17.2 ± 0.4	5.75 ± 0.12	1.4 ± 0.1	0.47 ± 0.03	0.1 ± 0.0	0.05 ± 0.01

which is a decisive parameter for the whole process; (2) the presence of biofilm, acting as cell retention, which is crucial to address the low growth rates and biomass yields of gas fermenting microbes; (3) the high gas-to-liquid mass transfer which characterizes TBRs, and ultimately enables a high flow of carbon and electrons from the syngas to the final products and last but not least (4) a Hydraulic Retention Time that allowed accumulation of acids in the system irrespectively of the gas flow rate and volume of the active TBR column. Only one study reviewed obtained higher productivities (2.6 g L^{-1} day^{-1} butyric and 1.23 g L^{-1} day^{-1} caproic acid) than the present study [28], using a co-culture of *C. ljungdahlii* and *C. Kluyveri* in a CSTR, maybe thanks to the integration of in-line extraction methods with the fermentation process, which could pull from the chain elongation reaction by extracting the products; or the use of a more reduced and CO rich syngas mix and higher syngas flows. Nevertheless, the lower HRT (1 day) used by Richter et al. [28], resulted also in lower butyric and caproic acid titers (2.7 g L^{-1} and 1.3 g L^{-1}) and yields (18 % carbon present in butyric, and 9 % present in caproic acid, vs 26 % and 25 %, respectively, in the case of the present study). All other studies reviewed for continuous syngas fermentation processes stayed at titers below 1.5 g L^{-1} butyric and 1 g L^{-1} caproic acid, and productivities below 0.75 g L-1 day butyric and 0.5 g L-1 day-1 caproic acid [15,41,42]. It is important to mention that the present study focuses solely on the pH effect, so that further optimization of the process may reach even higher titers and productivities of C4 & C6 acids. The TBR set-ups and operational conditions can be further optimised for mass transfer, while it is anticipated that experiments at bigger scale will further enhance productivities, due to the improved mass transfer [43,44]. Additionally, data from the pH 7.5 condition (Table 1) shows the potential of TBR for the production of acetic acid from syngas, which could be further enhanced by tuning pH, HRT, temperature, and syngas composition.

Despite the conversion of syngas to butyric and caproic acid was maximized at pH 6, around 40 % of the reducing equivalents were still found in acetic acid, one of the intermediate products. Acetic acid is one of the main products of acetogenesis, and in order to be converted into chain-elongated products, it needs ethanol. (reaction 4). Ethanol is produced via the Wood-Ljungdahl pathway directly from syngas or via reduction of acetic acid. In our process, ethanol is presumably simultaneously produced from syngas, and consumed to produce butyric and caproic acid. Here, a low ethanol-to-acetate ratio produced in the acetogenic step could be the reason for the reducing equivalents found in acetic acid. Therefore, strategies targeting an improvement of this ratio, such as more reducing syngas mixtures, should be the next rational step to improve the yields of butyric and caproic acid. Alternatively, external ethanol addition to syngas fermentation processes has already been proved successful in co-culture studies, achieving concentrations of butyric and caproic acid of 7 and 8.2 g L^{-1} in batch reactors [45]. Nonetheless, external ethanol addition could prove more challenging in mixed culture studies, since ethanol could also be directed to competing routes [46] such as acetogenesis [47] and sulfate reduction [48].

3.2. Microbial community analysis

The bacterial community was analysed at each of the steady-states reached, with samples coming from both suspended and attached microbes. The diversity of the bacterial community proved to be very constrained, as a total of merely 578 ASVs (amplicon sequence variant, i.e. each distinct DNA sequence in the 16S rDNA analysis) were obtained

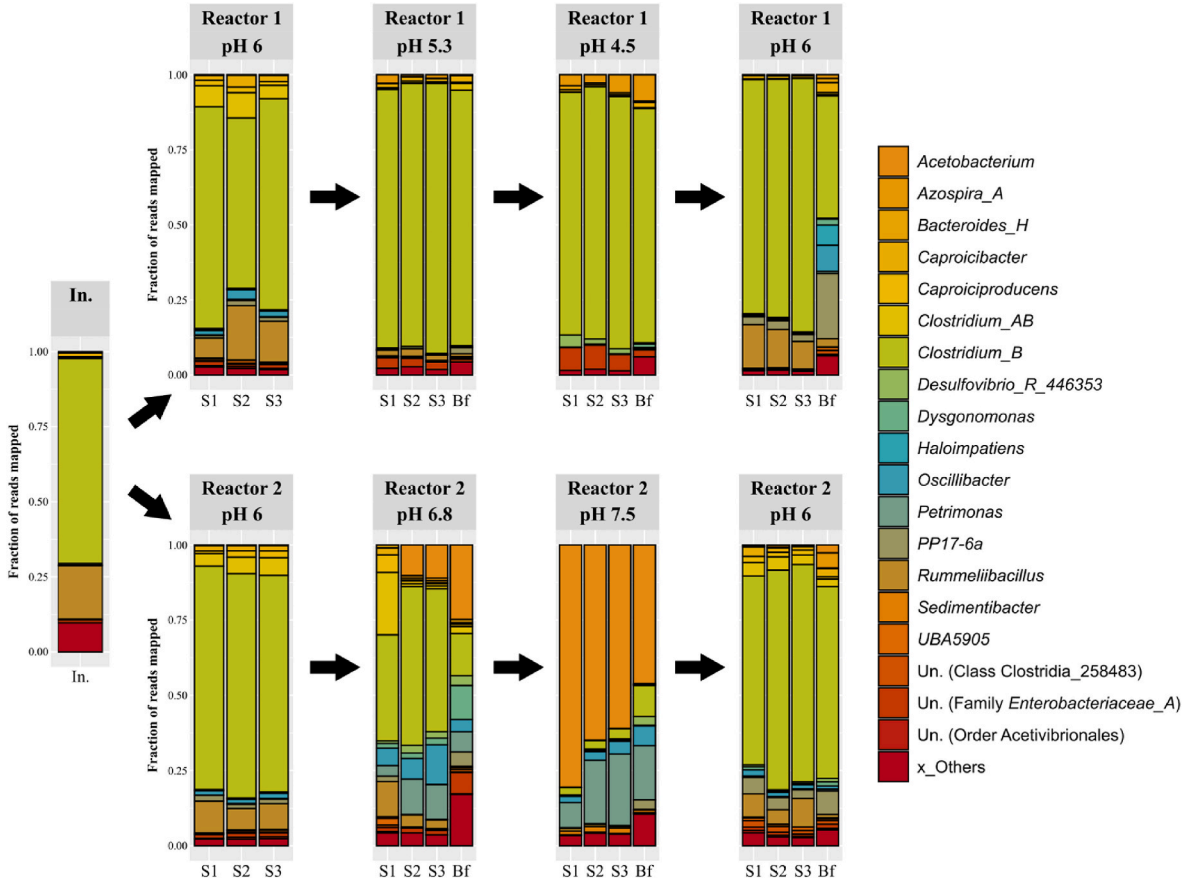

Fig. 4. Relative abundance of microbes, identified at genus level for the inoculum used, and each of the steady-states reached. The 19 most abundant genera are shown, while the rest were merged into "Others", also shown in the graph. Triplicates were taken of the suspended growth (S1, S2, and S3) for every steady-state, and biofilm samples (Bf) were also analysed for all except the initial pH 6 steady-states.

in the analysis. These were merged into 203 genera, out of which the 19 most abundant were plotted in Fig. 4. All conditions were dominated by one or two genera. From pH 4.5 to pH 6, the cultures were dominated by *Clostridium* spp., while at pH 7.5, *Acetobacterium* was the main genus. At pH 6.8 the community was the most diverse, with both *Clostridium* and *Acetobacterium* having a significant abundance (Fig. 4).

The biofilm samples did not show a notably different community than the suspended samples (Fig. 4), although a small increase in diversity was seen in some conditions (i.e. Reactor 1, final pH 6; Reactor 2, pH 6.8). This could be due to biofilm stratification, i.e. the existence of different functional guilds in the biofilm resulting from the heterogeneity of the conditions (e.g. pH, nutrients, and gas concentration gradients) [31]. Additionally, at pH 6, *Rummeliibacillus* was the second most abundant genus in the suspended growth samples, while in the biofilm samples it was replaced by *PP17-6a*, an unclassified genus within the Clostridia class.

Interestingly, although decreasing the pH from pH 6 to pH 5.3 and 4.5 did not have a significant effect on the bacterial community (Fig. 4, Reactor 1), it did impact both the product distribution and gas consumption of the TBRs (Fig. 2 A and C, and Fig. 3). It was, in fact, the same ASV which was the dominant through the whole pH 4.5 to pH 6 range. Therefore, the inhibition of chain elongation, the appearance of ethanol as a final product, and the drop in gas consumption, seen when lowering the pH, seemed to respond to intracellular metabolic regulation, more than to a change in the dominant microbes. Nevertheless, lowering the pH reduced significantly the relative abundance of *Rummeliibacillus*, a genus which has been associated with chain elongation and caproic acid production [49,50], and could therefore also have influenced the reactor performance. On the other hand, increasing the pH above pH 6 did have a significant effect in the microbial community distribution and this could therefore have been the main driver of the changes seen in the performance at this pH. pH 6.8 exhibited a decrease of *Clostridium* relative abundance, and the increase of genera such as *Acetobacterium*, *Oscillibacter*, and *Petrimonas*, while increasing to pH 7.5, decreased the *Clostridium* genus relative abundance even further and *Acetobacterium* became the dominant genus. pH 6 seemed therefore to be the most favourable pH for the *Clostridium* species present in this study, which was likely responsible for the overall conversion of H_2, CO, and CO_2 to acetic acid and ethanol, and subsequently to butyric and then caproic acid (together with *Rummeliibacillus*). In turn, pH 7.5 appeared to be the most favourable pH for the growth of *Acetobacterium* on syngas, though higher pH conditions than the ones tested in this study could potentially be more favourable, with the concomitant production of, predominantly, acetic acid.

Certain genera, known for their chain elongating potential, i.e. *Caproiciproducens* and *Caprocibacter* were also identified, at very low abundances. The response of their abundance was very similar to the response of *Rummeliibacillus*, i.e. it decreased with lowering pH, while operation at the higher pH of 7.5 exhibited the same effect. Reverting the operation to pH 6.0 restored the abundances of these chain elongating strain as well.

3.3. Robustness and reproducibility of trickle bed reactors

All the results shown, comparing the performance of TBRs at different pH conditions, were tested in two different reactors, so that different pH conditions were tested in each reactor, without replicates. Moreover, the different conditions tested were run sequentially by changing the set pH of the reactor, instead of starting each experiment with a new inoculum. Therefore, to ensure the robustness and reproducibility of the results, both reactors were started at a pH of 6, and after all the different pH conditions were tested, they were both returned to pH 6 again. In this way, the initial resemblance of the two reactors can be assessed, so pH conditions tested in different reactors can be compared as if they were tested in the same reactor. Additionally, by comparing the performance and the community at pH 6 at the beginning and the end of the study, for both reactors, it can be verified whether the performance of the reactor at a specific pH is independent of the pH conditions tested before in the reactor.

Fig. 5 illustrates the performance of the TBRs 1 and 2 at the pH 6 steady-states at the beginning and end of the study. The high similarity between reactors 1 and 2 at the beginning of the experiment, both in terms of the e-mol equivalents distribution in the products (Fig. 5A) and gas consumption (Fig. 5B), demonstrates both reactors started the experiment as duplicates. This is also observed in the production and consumption profile both reactors followed in the first 60 days of fermentation (Fig. 2). This similarity was again restored at the end of the study, in spite of the fact that TBR1 had been subjected to pH 5.3 and pH 4.5, while TBR2 had been running at pH 6.8 and pH 7.5.

A similar pattern was seen when comparing the microbial community in both reactors at the starting and ending pH 6 conditions (Fig. 4). Both reactors reached initially a community dominated by *Clostridium* genus, followed by a minor presence of *Rummeliibacillus*. As commented earlier, TBR1 did not exhibited a significant change in community when the pH was lowered to 5.3 first and then to 4.5 (besides the disappearance of *Rummeliibacillus)*, while in TBR2, at pH 7.5, *Acetobacterium* outcompeted *Clostridium*, which ended up representing less than 10 % of the total microbial abundance. However, after they were set back to pH 6, both reactors converged again to the same original community, with similar *Clostridium* and *Rummeliibacillus* relative abundances.

Overall, these results highlight the robustness of mixed-culture industrial fermentations, and demonstrate that, to a certain extent, the performance of these processes, can easily be recovered after adverse events greatly impacting the reactor. Further studies should determine whether this characteristic is exclusive of biofilm reactors, which can potentially maintain higher microbial diversities due to the wide spectrum of conditions existing within the biofilm, or on the other hand it is extendable to all suspended and attached mixed culture fermentations.

4. Conclusions

TBRs and undefined mixed culture fermentations proved to be a relevant approach for the conversion of syngas to C4 & C6 acids. The highest productivities and titers reached were 1.17 ± 0.10 g L^{-1} day^{-1} and 3.51 ± 0.29 g L^{-1} for butyric acid and 0.97 ± 0.05 g L^{-1} day^{-1} and 2.9 ± 0.15 g L^{-1} for caproic acid, respectively, at pH 6, which are the highest achieved to date in gas fermentation processes. At pH 6, 40 % of the available electrons in the products were found in acetic acid, while butyric and caproic acid comprised 29 % of the electrons each, meaning 58 % of the consumed electrons ended up in the target products. The 16S rDNA analysis showed that, at that pH, the acetogenic and chain elongating community was dominated by a single *Clostridium* species, followed by a species from the *Rummeliibacillus* genus. This study highlighted the role of pH in the simultaneous conversion of syngas to elongated acids in biofilm reactors, as the efficiency of the process dropped sharply at pH values of 5.3 and 6.8, aligning with studies performed with defined and undefined suspended mixed cultures. Lastly, all steady states achieved at pH 6 were identical in terms of microbial community, conversion efficiencies, and production profile regardless of whether they were reached directly after the reactors' start-up or after pH 4.5 or 7.5 operation, demonstrating thus the robustness of biofilm-based, mixed-culture fermentations in respect to pH changes.

CRediT authorship contribution statement

Cesar Quintela: Writing – original draft, Visualization, Methodology, Investigation, Formal analysis, Data curation, Conceptualization. **Antonio Grimalt-Alemany:** Writing – review & editing, Methodology, Investigation. **Oskar Modin:** Writing – review & editing, Formal analysis, Data curation. **Yvonne Nygård:** Writing – review & editing, Visualization, Supervision, Methodology, Investigation. **Lisbeth Olsson:** Writing – review & editing, Visualization, Supervision,

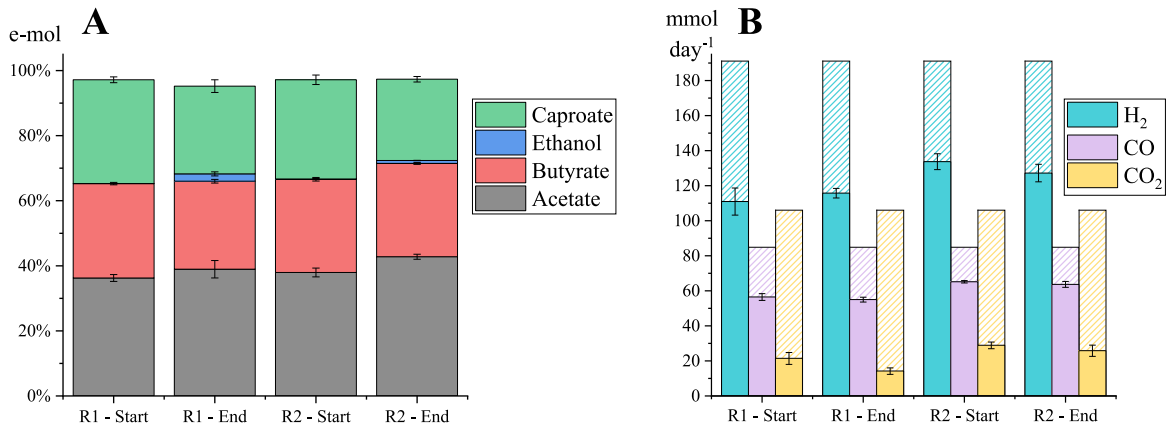

Fig. 5. Averaged e-mol distribution in the extracellular products (A) and consumption of the gaseous substrates in mmol day^{-1} (B) for each of the steady states reached at pH 6. In plot B, the total provided gases is given in a striped pattern, while the consumed portion is shown in a solid pattern. To derive volumetric gas consumption rates, the 0.3 L_{EBV} must be used.

Methodology, Investigation. **Ioannis V. Skiadas:** Writing – review & editing, Visualization, Supervision, Methodology, Investigation, Conceptualization. **Hariklia N. Gavala:** Writing – review & editing, Visualization, Supervision, Resources, Project administration, Methodology, Funding acquisition, Data curation, Conceptualization.

Declaration of competing interest

The authors declare that they have no known competing financial interests or personal relationships that could have appeared to influence the work reported in this paper.

Data availability

Data will be made available on request.

Acknowledgments

This study was supported by the DTU PhD alliance scheme and DTU Chemical Engineering.

Appendix A. Supplementary data

Supplementary data to this article can be found online at https://doi.org/10.1016/j.biombioe.2024.107292.

References

[1] H. Lee, J. Romero, C.W.T. Ipcc, Climate Change 2023: Synthesis Report. A Report of the Intergovernmental Panel on Climate Change. Contribution of Working Groups I, II and III to the Sixth Assessment Report of the Intergovernmental Panel on Climate Change, IPCC, Geneva, Switzerland, 2023, p. 24.
[2] A. Grimalt-Alemany, I.V. Skiadas, H.N. Gavala, Syngas biomethanation: state-of-the-art review and perspectives, Biofuels, Bioproducts and Biorefining 12 (2018) 139–158, https://doi.org/10.1002/bbb.1826.
[3] I.K. Stoll, N. Boukis, J. Sauer, Syngas fermentation to alcohols: reactor technology and Application perspective, Chem. Ing. Tech. 92 (2020) 125–136, https://doi.org/10.1002/cite.201900118.
[4] K. Asimakopoulos, M. Kaufmann-Elfang, C. Lundholm-Høffner, N.B.K. Rasmussen, A. Grimalt-Alemany, H.N. Gavala, I.V. Skiadas, Scale up study of a thermophilic trickle bed reactor performing syngas biomethanation, Appl. Energy 290 (2021), https://doi.org/10.1016/j.apenergy.2021.116771.
[5] B.D. Jønson, P. Tsapekos, M. Tahir Ashraf, M. Jeppesen, J. Ejbye Schmidt, J. R. Bastidas-Oyanedel, Pilot-scale study of biomethanation in biological trickle bed reactors converting impure CO2 from a Full-scale biogas plant, Bioresour. Technol. 365 (2022), https://doi.org/10.1016/j.biortech.2022.128160.
[6] D.C. Calvo, H.J. Luna, J.A. Arango, C.I. Torres, B.E. Rittmann, Determining global trends in syngas fermentation research through a bibliometric analysis, J. Environ. Manag. 307 (2022) 114522, https://doi.org/10.1016/j.jenvman.2022.114522.
[7] R. Kleerebezem, M.C. van Loosdrecht, Mixed culture biotechnology for bioenergy production, Curr. Opin. Biotechnol. 18 (2007) 207–212, https://doi.org/10.1016/j.copbio.2007.05.001.
[8] S. Wainaina, Lukitawesa, M. Kumar Awasthi, M.J. Taherzadeh, Bioengineering of anaerobic digestion for volatile fatty acids, hydrogen or methane production: a critical review, Bioengineered 10 (2019) 437–458, https://doi.org/10.1080/21655979.2019.1673937.
[9] C. Kourmentza, J. Plácido, N. Venetsaneas, A. Burniol-Figols, C. Varrone, H. N. Gavala, M.A.M. Reis, Recent advances and challenges towards sustainable polyhydroxyalkanoate (PHA) production, Bioengineering 4 (2017), https://doi.org/10.3390/bioengineering4020055.
[10] H.N. Gavala, A. Grimalt-Alemany, K. Asimakopoulos, I.V. Skiadas, Gas biological conversions: the potential of syngas and carbon dioxide as production platforms, Waste Biomass Valorization 12 (2021) 5303–5328, https://doi.org/10.1007/s12649-020-01332-7.
[11] S. Wirth, P. Dürre, Investigation of putative genes for the production of medium-chained acids and alcohols in autotrophic acetogenic bacteria, Metab. Eng. 66 (2021) 296–307, https://doi.org/10.1016/j.ymben.2021.04.010.
[12] H.J. Oh, G. Gong, J.H. Ahn, J.K. Ko, S.M. Lee, Y. Um, Effective hexanol production from carbon monoxide using extractive fermentation with Clostridium carboxidivorans P7, Bioresour. Technol. 367 (2023), https://doi.org/10.1016/j.biortech.2022.128201.
[13] J. Kim, K.Y. Kim, J.K. Ko, S.M. Lee, G. Gong, K.H. Kim, Y. Um, Characterization of a novel acetogen Clostridium sp. JS66 for production of acids and alcohols: focusing on hexanoic acid production from syngas, Biotechnol. Bioproc. Eng. 27 (2022) 89–98, https://doi.org/10.1007/s12257-021-0122-1.
[14] J. Daniell, M. Köpke, S.D. Simpson, Commercial biomass syngas fermentation, Energies 5 (2012) 5372–5417, https://doi.org/10.3390/en5125372.
[15] M. Diender, I. Parera Olm, M. Gelderloos, J.J. Koehorst, P.J. Schaap, A.J.M. Stams, D.Z. Sousa, Metabolic shift induced by synthetic co-cultivation promotes high yield of chain elongated acids from syngas, Sci. Rep. 9 (2019), https://doi.org/10.1038/s41598-019-54445-y.
[16] Y.Q. Wang, F. Zhang, W. Zhang, K. Dai, H.J. Wang, X. Li, R.J. Zeng, Hydrogen and carbon dioxide mixed culture fermentation in a hollow-fiber membrane biofilm reactor at 25 °C, Bioresour. Technol. 249 (2018) 659–665, https://doi.org/10.1016/j.biortech.2017.10.054.
[17] W. De Araújo, R. Carrhá, T.A. Gehring, L.T. Angenent, S. Tédde, Anaerobic fermentation for n- caproic acid production : a review, Process Biochem. 54 (2017) 106–119, https://doi.org/10.1016/j.procbio.2016.12.024.
[18] M. Roghair, Y. Liu, J.C. Adiatma, R.A. Weusthuis, M.E. Bruins, C.J.N. Buisman, D. P.B.T.B. Strik, Effect of n-caproate concentration on chain elongation and competing processes, ACS Sustain. Chem. Eng. 6 (2018) 7499–7506, https://doi.org/10.1021/acssuschemeng.8b00200.
[19] C. Quintela, E. Peshkepia, A. Grimalt-Alemany, Y. Nygard, L. Olsson, I. V Skiadas, H.N. Gavala, Excessive ethanol oxidation versus efficient chain elongation processes, Waste Biomass Valorization 15 (2024) 2545–2558, https://doi.org/10.1007/s12649-023-02323-0.
[20] F. Liew, A.M. Henstra, M. Köpke, K. Winzer, S.D. Simpson, N.P. Minton, Metabolic engineering of Clostridium autoethanogenum for selective alcohol production, Metab. Eng. 40 (2017) 104–114, https://doi.org/10.1016/j.ymben.2017.01.007.
[21] A. Grimalt-Alemany, M. Łężyk, L. Lange, I. V Skiadas, H.N. Gavala, Enrichment of syngas-converting mixed microbial consortia for ethanol production and thermodynamics-based design of enrichment strategies, Biotechnol. Biofuels 11 (2018) 1–22, https://doi.org/10.1186/s13068-018-1189-6.
[22] H. Richter, B. Molitor, H. Wei, W. Chen, L. Aristilde, L.T. Angenent, Ethanol production in syngas-fermenting: Clostridium ljungdahlii is controlled by thermodynamics rather than by enzyme expression, Energy Environ. Sci. 9 (2016) 2392–2399, https://doi.org/10.1039/c6ee01108j.

[23] K. Valgepea, R. de Souza Pinto Lemgruber, K. Meaghan, R.W. Palfreyman, T. Abdalla, B.D. Heijstra, J.B. Behrendorff, R. Tappel, M. Köpke, S.D. Simpson, L. K. Nielsen, E. Marcellin, Maintenance of ATP homeostasis triggers metabolic shifts in gas-fermenting acetogens, Cell Syst 4 (2017) 505–515.e5, https://doi.org/10.1016/j.cels.2017.04.008.

[24] H.N. Abubackar, Á. Fernández-Naveira, M.C. Veiga, C. Kennes, Impact of cyclic pH shifts on carbon monoxide fermentation to ethanol by Clostridium autoethanogenum, Fuel 178 (2016) 56–62, https://doi.org/10.1016/j.fuel.2016.03.048.

[25] R. Ganigué, P. Sánchez-Paredes, L. Bañeras, J. Colprim, Low fermentation pH is a trigger to alcohol production, but a killer to chain elongation, Front. Microbiol. 7 (2016) 702, https://doi.org/10.3389/FMICB.2016.00702/BIBTEX.

[26] P. San-Valero, H.N. Abubackar, M.C. Veiga, C. Kennes, Effect of pH, yeast extract and inorganic carbon on chain elongation for hexanoic acid production, Bioresour. Technol. 300 (2020) 122659, https://doi.org/10.1016/J.BIORTECH.2019.122659.

[27] H. Richter, B. Molitor, H. Wei, W. Chen, L. Aristilde, L.T. Angenent, Ethanol production in syngas-fermenting: Clostridium ljungdahlii is controlled by thermodynamics rather than by enzyme expression, Energy Environ. Sci. 9 (2016) 2392–2399, https://doi.org/10.1039/c6ee01108j.

[28] H. Richter, B. Molitor, M. Diender, D.Z. Sousa, L.T. Angenent, A narrow pH range supports butanol, hexanol, and octanol production from syngas in a continuous co-culture of Clostridium ljungdahlii and Clostridium kluyveri with in-line product extraction, Front. Microbiol. 7 (2016), https://doi.org/10.3389/fmicb.2016.01773.

[29] M. Diender, A.J.M. Stams, D.Z. Sousa, Production of medium-chain fatty acids and higher alcohols by a synthetic co-culture grown on carbon monoxide or syngas, Biotechnol. Biofuels 9 (2016), https://doi.org/10.1186/s13068-016-0495-0.

[30] K. Asimakopoulos, H.N. Gavala, I.V. Skiadas, Reactor systems for syngas fermentation processes: a review, Chem. Eng. J. 348 (2018) 732–744, https://doi.org/10.1016/j.cej.2018.05.003.

[31] P.S. Stewart, M.J. Franklin, Physiological heterogeneity in biofilms, Nat. Rev. Microbiol. 6 (2008) 199–210, https://doi.org/10.1038/nrmicro1838.

[32] N. Birger Ramsing, M. Kuhl, B.J. Barker, Distribution of sulfate-reducing bacteria, 02, and H2S in photosynthetic biofilms determined by oligonucleotide probes and microelectrodes. https://journals.asm.org/journal/aem, 1993.

[33] D. De Beer, J.W. Huisman, J.C. Van Den Heuvel, S.P.P. Or, THE EFFECT OF AGGREGATES pH PROFILES IN METHANOGENIC ON THE KINETICS OF ACETATE CONVERSION, 1992.

[34] A. Grimalt-Alemany, C. Etler, K. Asimakopoulos, I.V. Skiadas, H.N. Gavala, ORP control for boosting ethanol productivity in gas fermentation systems and dynamics of redox cofactor NADH/NAD+under oxidative stress, J. CO2 Util. 50 (2021), https://doi.org/10.1016/j.jcou.2021.101589.

[35] K. Asimakopoulos, H.N. Gavala, I.V. Skiadas, Biomethanation of syngas by enriched mixed anaerobic consortia in trickle bed reactors, Waste Biomass Valorization 11 (2020) 495–512, https://doi.org/10.1007/s12649-019-00649-2.

[36] A. Grimalt-Alemany, M. Łężyk, L. Lange, I.V. Skiadas, H.N. Gavala, Enrichment of syngas-converting mixed microbial consortia for ethanol production and thermodynamics-based design of enrichment strategies, Biotechnol. Biofuels 11 (2018), https://doi.org/10.1186/s13068-018-1189-6.

[37] Apha, Standard Methods for the Examination of Water and Wastewater, Apha, 1985.

[38] W. Walters, E.R. Hyde, D. Berg-Lyons, G. Ackermann, G. Humphrey, A. Parada, J. A. Gilbert, J.K. Jansson, J.G. Caporaso, J.A. Fuhrman, Improved bacterial 16S rRNA gene (V4 and V4-5) and fungal internal transcribed spacer marker gene primers for microbial community surveys, mSystems 1 (2016) e00009, 15.

[39] E. Bolyen, J.R. Rideout, M.R. Dillon, N.A. Bokulich, C.C. Abnet, G.A. Al-Ghalith, H. Alexander, E.J. Alm, M. Arumugam, F. Asnicar, Y. Bai, J.E. Bisanz, K. Bittinger, A. Brejnrod, C.J. Brislawn, C.T. Brown, B.J. Callahan, A.M. Caraballo-Rodríguez, J. Chase, E.K. Cope, R. Da Silva, C. Diener, P.C. Dorrestein, G.M. Douglas, D. M. Durall, C. Duvallet, C.F. Edwardson, M. Ernst, M. Estaki, J. Fouquier, J. M. Gauglitz, S.M. Gibbons, D.L. Gibson, A. Gonzalez, K. Gorlick, J. Guo, B. Hillmann, S. Holmes, H. Holste, C. Huttenhower, G.A. Huttley, S. Janssen, A. K. Jarmusch, L. Jiang, B.D. Kaehler, K. Bin Kang, C.R. Keefe, P. Keim, S.T. Kelley, D. Knights, I. Koester, T. Kosciolek, J. Kreps, M.G.I. Langille, J. Lee, R. Ley, Y. X. Liu, E. Loftfield, C. Lozupone, M. Maher, C. Marotz, B.D. Martin, D. McDonald, L.J. McIver, A.V. Melnik, J.L. Metcalf, S.C. Morgan, J.T. Morton, A.T. Naimey, J. A. Navas-Molina, L.F. Nothias, S.B. Orchanian, T. Pearson, S.L. Peoples, D. Petras, M.L. Preuss, E. Pruesse, L.B. Rasmussen, A. Rivers, M.S. Robeson, P. Rosenthal, N. Segata, M. Shaffer, A. Shiffer, R. Sinha, S.J. Song, J.R. Spear, A.D. Swafford, L. R. Thompson, P.J. Torres, P. Trinh, A. Tripathi, P.J. Turnbaugh, S. Ul-Hasan, J.J. J. van der Hooft, F. Vargas, Y. Vázquez-Baeza, E. Vogtmann, M. von Hippel, W. Walters, Y. Wan, M. Wang, J. Warren, K.C. Weber, C.H.D. Williamson, A. D. Willis, Z.Z. Xu, J.R. Zaneveld, Y. Zhang, Q. Zhu, R. Knight, J.G. Caporaso, Reproducible, interactive, scalable and extensible microbiome data science using QIIME 2, Nat. Biotechnol. 37 (8 37) (2019) 852–857, https://doi.org/10.1038/s41587-019-0209-9, 2019.

[40] C.M. Spirito, H. Richter, K. Rabaey, A.J.M. Stams, L.T. Angenent, Chain elongation in anaerobic reactor microbiomes to recover resources from waste, Curr. Opin. Biotechnol. 27 (2014) 115–122, https://doi.org/10.1016/j.copbio.2014.01.003.

[41] H.J. Wang, K. Dai, Y.Q. Wang, H.F. Wang, F. Zhang, R.J. Zeng, Mixed culture fermentation of synthesis gas in the microfiltration and ultrafiltration hollow-fiber membrane biofilm reactors, Bioresour. Technol. 267 (2018) 650–656, https://doi.org/10.1016/j.biortech.2018.07.098.

[42] N. Shen, K. Dai, X.Y. Xia, R.J. Zeng, F. Zhang, Conversion of syngas (CO and H2) to biochemicals by mixed culture fermentation in mesophilic and thermophilic hollow-fiber membrane biofilm reactors, J. Clean. Prod. 202 (2018) 536–542, https://doi.org/10.1016/j.jclepro.2018.08.162.

[43] S. Dutta, H.N. Gavala, I. V Skiadas, Expressing variable mass transfer coefficients for gas fermentation in trickle bed reactor, Chem. Eng. J. 475 (2023), https://doi.org/10.1016/j.cej.2023.146086.

[44] S. Dutta, M. Krikeli, H.N. Gavala, I.V. Skiadas, Dynamic tank-in series modelling and simulæation of gas-liquid interaction in trickle bed reactor designed for gas fermentation, J. Clean. Prod. (2024).

[45] C. Fernández-Blanco, M.C. Veiga, C. Kennes, Efficient production of n-caproate from syngas by a co-culture of Clostridium aceticum and Clostridium kluyveri, J. Environ. Manag. 302 (2022) 113992, https://doi.org/10.1016/J.JENVMAN.2021.113992.

[46] C. Quintela, E. Peshkepia, A. Grimalt-Alemany, Y. Nygård, L. Olsson, I. V Skiadas, H. Gavala, Waste and Biomass Valorization Excessive ethanol oxidation versus efficient chain elongation processes, Waste Biomass Valorization (2023), https://doi.org/10.1007/978-1-4612-1072.

[47] J. Bertsch, A.L. Siemund, F. Kremp, V. Müller, A novel route for ethanol oxidation in the acetogenic bacterium Acetobacterium woodii: the acetaldehyde/ethanol dehydrogenase pathway, Environ. Microbiol. 18 (2016) 2913–2922, https://doi.org/10.1111/1462-2920.13082.

[48] D.R. Kremer, H.E. Nienhuis-Kuiper, T.A. Hansen, Ethanol dissimilation in desulfovibrio, Arch. Microbiol. 150 (1988) 552–557.

[49] B. Wu, R. Lin, X. Ning, X. Kang, C. Deng, A.D.W. Dobson, J.D. Murphy, An assessment of how the properties of pyrochar and process thermodynamics impact pyrochar mediated microbial chain elongation in steering the production of medium-chain fatty acids towards n-caproate, Bioresour. Technol. 358 (2022) 127294, https://doi.org/10.1016/j.biortech.2022.127294.

[50] C. Liu, Y. Du, J. Zheng, Z. Qiao, H. Luo, W. Zou, Production of caproic acid by Rummeliibacillus suwonensis 3B-1 isolated from the pit mud of strong-flavor baijiu, J. Biotechnol. 358 (2022) 33–40, https://doi.org/10.1016/J.JBIOTEC.2022.08.017.